

Echo power calculation mathematical model and signal processing method of laser fuze based on circumferential detection mechanism

JIE WU*

School of Defense, Xi'an Technological University, Xi'an 710021, China

To improve the detection performance of the pulse laser fuze circumferential detection system, this paper studies the echo characteristics of pulse laser fuze circumferential detection system and the adaptive filtering method of the echo signal under the cloud and fog environment. Based on the working principle of laser fuze and the constraint conditions that the system can detect ground targets, the calculation functions for the minimum scanning frequency of laser circumferential detection and the minimum pulse frequency of pulse laser are established; Due to the influence of cloud and fog environment on the echo signal, an adaptive filtering method is used to filter out interference signals and restore the real echo signal detected by the system. By integrating the detection model of the system for ground target, the echo power calculation mathematical model is derived using the bidirectional reflection distribution function. The filtering effect of adaptive filtering method on echo signals under different external interference factors, as well as the detection probability of the system under different motor scanning frequencies and laser pulse frequencies, were simulated and analyzed. The results demonstrate the feasibility of proposing the mathematical model and signal processing method in this paper.

(Received June 2, 2023; accepted October 9, 2023)

Keywords: Laser circumferential detection, Laser fuze, Echo power, Adaptive filtering, Detection probability

1. Introduction

Pulse laser has a small divergence angle, short pulse duration, concentrated energy, and has a large instantaneous power, applying the pulse laser as a fuze to detect target can ensure the reliable detection ability of the laser fuze detection system, therefore, it has been widely used in conventional ammunition and missiles [1-3]. To achieve functionalities such as a wide field of view, precise positioning, and accurate detonation control in laser proximity fuze, a synchronized scanning approach utilizing laser emission and reception systems is employed to detect the target, this approach forms a high-speed rotating scanning system, improving the possibility of laser beam scanning to detect targets and constituting a 360° circumferential detection system, thereby expanding the coverage range of target detection. Some scholars have conducted relevant researches on laser circumferential scanning detection method, Zhang et al. [4] established a detection model for ground targets at ultra-low altitudes using a circumferential laser fuze, derived the ground target echo power equation received by the laser fuze in the time domain according to the bidirectional reflection distribution function, calculated and analyzed the laser echo parameters under various conditions, including missile flight altitude, missile pitch attitude, and ground reflection characteristics. Zha et al. [5] studied the detection probability of single beam expansion scanning laser circumferential detection system, derived the calculation functions of minimum scanning frequency and

laser pulse frequency, and analyzed the effects of pulse frequency, laser beam angle, and beam incidence angle on the detection capability of the system for different diameter targets. Xu et al. [6] proposed a projectile-target intersection model for the circumferential detection system, adopted the Monte Carlo algorithm to analyze the influence of laser pulse frequency and motor scanning speed on the target detection probability of the system, and obtained the optimal pulse frequency and motor scanning speed. Yao et al. [7] presented a projectile-target intersection model utilizing spatial analytic geometry methods, established a detection probability model for projectile-target intersection based on the Monte Carlo method, and analyzed the detection probability of the system under different rocket velocities, target velocities, laser pulse frequencies, and detection radius. Zhang et al. [8] put forward an optimal detonation model for synchronized scanning pulse laser proximity fuze, analyzed the azimuth, distance, and positional coordinates of multiple detection points during the projectile-target intersection process, derived the target's velocity calculation model based on multiple detection points, and obtained the optimal detonation time and position information by calculating the target's velocity to distinguish between true and false targets. Ni et al. [9] utilized a high-speed rotating platform and a plane mirror to simulate the laser fuze, the laser beam of the stationary laser fuze is transformed into a beam that simulates high-speed passing of the target during the process-target intersection, and calculated the scanning speed and

effective distance. Meng et al. [10] studied the detection capability of the laser detection system for target echo signals under sea conditions, analyzed the effects of the field of view angle and incident angle parameters of the system on the characteristics of the sea surface echo, compared and analyzed the laser echo characteristics of wide-field-of-view and narrow-field-of-view under different sea conditions. Chen et al. [11] employed a laser fuze fixed-distance and detonation point control accuracy testing device with isokinetic spiral target, simulated the process of laser fuze forward fixed distance fuze approaching the target at high speed, this process is used to equivalent the projectile-target intersection state during the forward fixed distance fuze action of the laser fuze. Feng et al. [12] established a projectile-target intersection model by based on FPGA-based target azimuth discrimination and anti-interference strategies, and analyzed the target capture rate. The interference of clouds and fog in the environment has a significant impact on the detection of targets by laser fuzes, primarily due to the similarity in particle diameter and pulse laser wavelength, leading to optical effects such as Mie scattering, which alter the characteristics of laser echo signals including amplitude and pulse width, thereby affecting the precision of laser fuze short-range detection system. Higuchi et al. [13] employed narrow pulse laser emission techniques to reduce the effect of particle backscattered echo overlap and decrease the power of echo interference signals. Apart from the impact caused by shielded backscattering on the detection system, these filtering methods can be adopted to eliminate the effect of backscattering on the echo signals. Cheng et al. [14] developed a variable forgetting factor recursive least squares adaptive filtering algorithm, which effectively filters out backscattered signals, however, the high filter order of 400-500 results in substantial computational cost.

In this paper, we investigate the detection performance of the dual-transmitter and dual-receiver laser

fuze circumferential detection system; the research achievement can provide a basis for laser reliable detection in complex environments. The main contributions of this work are as follows:

(1) The calculation models of minimum scanning frequency and pulse frequency under the projectile-target intersection state are established, and the constraint function of the ground target detected by the system is constructed.

(2) Considering the influence of Mie scattering on the backscattering of pulsed laser in cloud and fog environments, a variable step-size adaptive filtering method is put forward to suppress the interference of cloud and fog echo signals on target signals.

(3) The echo power calculation mathematical model is set up according to the bidirectional reflectance distribution function of the target's surface.

The remainder of this paper is organized as follows. The working principle of dual-transmitter and dual-receiver laser fuze circumferential detection system is detailed in section 2. Laser fuze circumferential detection model is described in section 3. Laser circumferential detection echo signal processing method and echo power calculation mathematical model is described in section 4. Section 5 gives the calculation and analysis. Finally, Section 6 concludes the paper.

2. Dual-transmitter and dual-receiver laser fuze circumferential detection system

In order to effectively intercept the ground target attacked by the projectile, the laser fuze needs to possess a 360° omni-directional detection capability. In this paper, a dual-transmitter dual-receiver laser fuze circumferential detection system is employed to detect the ground targets using laser fuze. The schematic diagram of working principle of the system is shown in Fig. 1.

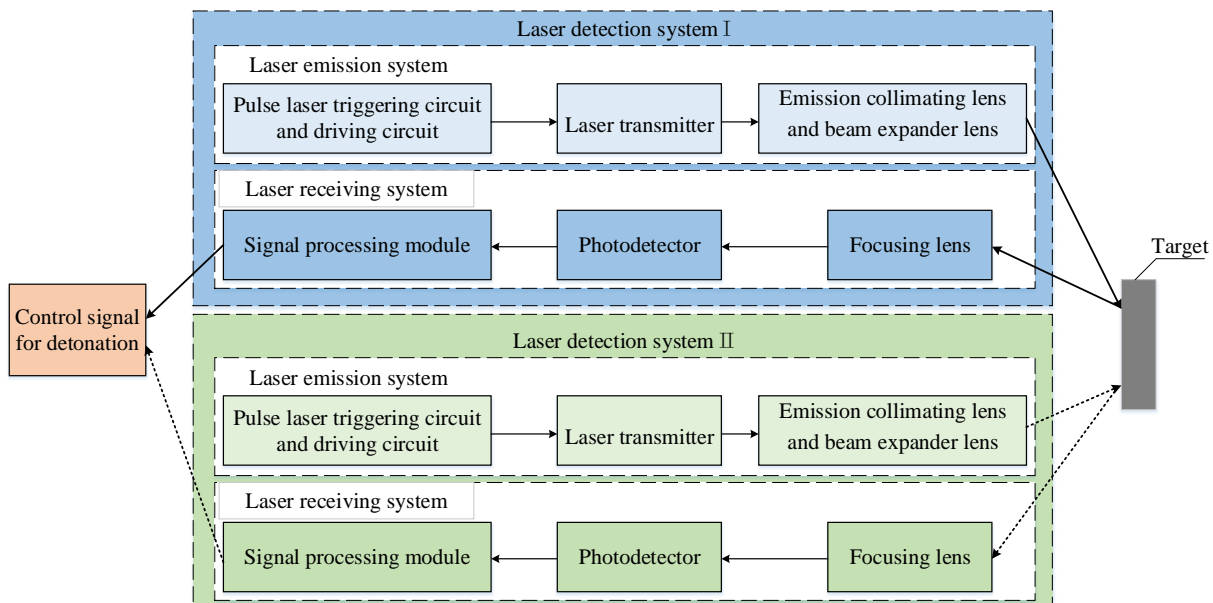


Fig. 1. Schematic diagram of working principle of dual-transmitter and dual-receiver laser fuze circumferential detection system (color online)

In Fig. 1, laser detection systems I and II are uniformly arranged around the fuze head, each laser detection system consists of laser emission system and laser receiving system, laser emission system consists of pulse laser triggering circuit and driving circuit, laser transmitter, emission collimating lens and beam expander lens, laser receiving system consists of focusing lens, photodetector and signal processing module. The laser beam emitted by the laser transmitter is directed onto the target through the emission collimating lens and beam expander lens. The laser receiving system captures the echo beam reflected or scattered by the target, which is then converged onto the photodetector through the focusing lens, after being output control signal by the signal processing module. The photodetector is installed in the fuze head, starts operating when provided with electrical power by the circuit control system. The two laser transmitters emit laser beams that form detection beams through optical lenses. The rotation of the fuze head's rotor converts the two detection beams into cone-shaped detection area. When the system detects the ground target, the target echo signal is provided to the circuit control system as the control signal for fuze detonation. The laser beams emitted begin working when electrical power is supplied by the circuit, upon encountering the target, a portion of the laser is reflected back into the laser receiver. The laser beams, rotating with the projectile, possess the capability of omnidirectional scanning to detect target. The laser beam that rotates with the projectile has the ability to scan and detect the target in all directions. When the circuit provides electrical energy, the fuze begins to work, the emitted laser beam encounters the target, and it returns some of the laser energy and enters the photodetector. In order to increase the detection field of view of the system, the photodetector is formed by splicing multiple unit detectors in a strip arrangement [15-17]. During the circumferential detection process, any one of the laser detection systems I and II detects a target, once the target echo signal meets the system's detonation conditions, outputting an detonation control signal.

During the detection process of the system for ground target, the pulse laser generates pulse signals that drive the laser through amplification to form pulsed laser beams. These pulsed laser beams are emitted outward through the emission optical system, while the timing is initiated. The reflected beam propagates through the air and forms a reflection beam when encountering a target on the ground. The reflected laser beam enters the receiving optical system, where it is focused onto the receiving plane of the photodetector. The photodetector outputs a weak electrical signal after converting the optical signal to electrical. The signal processing module amplifies and converts the weak electrical signal, and the arrival time of the target echo is determined by the time identification circuit, which provides a stop timing signal. The distance between the laser fuze and the target can be calculated based on the obtained timing information. With the acquired distance information and the target signal recognition criteria, the identification of the target is completed. According to the

requirements of fuze-warhead coordination, an ignition command is issued.

3. Laser fuze circumferential detection model

3.1. Calculation models for minimum scanning frequency and pulse frequency

The pulse fuze circumferential detection mode exists the periodic detection blind area, only when the scanning frequency is fast enough, the generated blind area will not significantly affect the detection performance of the system. At the same time, the adoption of pulse laser detection results in intermittent detection blind area in time, which needs to be improved by increasing the pulse frequency. Based on the detection principle of dual-transmitter and dual-receiver circumferential scanning mode, multiple laser beams form a circumferential beam field within one scanning cycle. A schematic diagram of the pulse laser beams within one scanning cycle, as observed from a top-down perspective, is shown in Fig. 2.

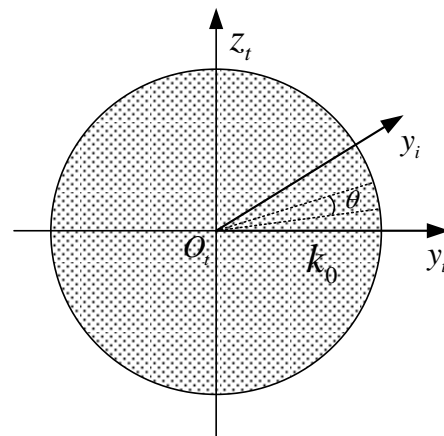


Fig. 2. The schematic diagram of pulse laser beams within one scanning cycle

In Fig. 2, the summation of the beam areas of pulse laser emission in one scanning cycle is represented by 2π . Due to the adoption of the dual-transmitter and dual-receiver mode, when designing the scanning frequency and pulse frequency, the integer multiples of the single laser beam angular displacement should be equal to $m\theta = \pi$, indicating the presence of $2m$ laser beams within one cycle.

To enhance the detection performance of the system, the system adopts a pulse laser with a duty cycle k significantly smaller than 1%. The time interval between two consecutive pulse lasers is denoted by t , $t = (1-k)T_f$, and T_f is the period of the pulse laser. Thus, the period of the pulse laser is utilized as the time interval between adjacent pulse lasers [18-19]. If the scanning frequency of the system is n and the pulse

frequency of the laser is f , the angle traversed between adjacent pulse lasers is given by formula (1).

$$\theta = \pi n T_f = \pi n / f \quad (1)$$

The angle between adjacent laser beams is referred to as the minimum angular resolution of the target azimuth recognition laser detection system, indicating the smallest angle that the system can distinguish. In the system, the design of the pulse frequency f is an integer multiple of the scanning frequency n . To ensure that no target is missed within a single scanning cycle, it is necessary to have at least m_{\min} laser beams, as shown in formula (2).

$$m_{\min} = \pi / \theta_{\max} \quad (2)$$

When the angle between the emitted laser beam and the projectile direction is equal to the angle between the target direction and the laser beam, the minimum scanning frequency is given by formula (3).

$$n_{\min} = (v_t + v_m) / L_t \quad (3)$$

where, v_t represents the projectile's velocity, v_m represents the target's velocity, and L_t represents the length of the target. The minimum pulse frequency is represented by formula (4).

$$f_{\min} = \pi n_{\min} / \theta_{\max} \quad (4)$$

The lowest scanning frequency of the laser system can be calculated when the size and velocity of the target detected by the system are determined. Combined with the known double-sending and double-receiving mode of the system, the maximum angle of rotation between the adjacent pulsed lasers is determined, and then the minimum pulse frequency of the laser is determined. The velocity of the detected target affects the scanning frequency of the system, which in turn also affects the pulse frequency of the laser. The main purpose of determining these parameters is to ensure that the system detects the target during a single scan cycle.

3.2. Projectile-target intersection model

The spatial position of the emitted laser beam in the system is determined by the projectile's rotational speed ω , pulse frequency f , and launch elevation angle α . Fig. 3 illustrates the schematic diagram of projectile-target intersection, where a projectile coordinate system $O_t x_t y_t z_t$ is established along the projectile axis. The pitch angle φ represents the inclination of the flying projectile, and the yaw angle β represents its deviation.

The laser beam's initial scanning beam is k_0 , and k'_0 is the projection of k_0 in plane $O_t z_t y_t$. After half a revolution, the laser beam k'_0 is formed. Due to the adoption of the dual-transmitter and dual-receiver mode, both laser beams rotate for half a cycle to form a 360° omni-directional detection area. The initial launch position of the laser beam coincides with the origin O_t of the projectile coordinate system and rotates around the axis x_t .

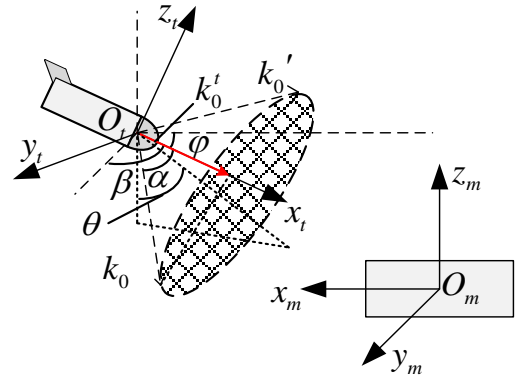


Fig. 3. The schematic diagram of projectile-target intersection

Assuming that axis $O_t y_t$ rotates around axis $O_m x_m$ with a projectile rotational speed of ω to reach angle $\pi \text{ rad}$ at position $O_m k'$, the linear equations of all scanning laser beams at time t are expressed as formula (5).

$$\begin{bmatrix} x_i \\ y_i \\ z_i \end{bmatrix} = \begin{bmatrix} \sin \alpha \sin(\omega t + \pi i) \\ \cos \alpha \\ \sin \alpha \cos(\omega t + \pi i) \end{bmatrix} l_i, i = 0, 1 \quad (5)$$

where (x_i, y_i, z_i) represents the spatial three-dimensional coordinate information of a specific point on the i -th laser beam, and l_i denotes the distance between a specific point on the i -th laser beam and the origin O_t of the projectile coordinate system.

Under the condition of the imminent intersection between the projectile and the ground target, the projectile and the ground target assume a head-on intersection posture. Based on the defined projectile coordinate system $O_t x_t y_t z_t$ and the ground target coordinate system $O_m x_m y_m z_m$, as well as the pitch angle φ and yaw angle β of the projectile in this posture, neglecting the

roll angle of the projectile at the moment of intersection, a transformation matrix from the projectile coordinate system to the ground target coordinate system is established, as shown in formula (6).

$$Q = \begin{bmatrix} \cos \varphi \cos \beta & -\cos \varphi \sin \beta & \sin \beta \\ \sin \varphi \cos \beta & \cos \varphi \sin \beta & 0 \\ -\sin \varphi \sin \beta & \sin \varphi \cos \beta & \cos \beta \end{bmatrix} \quad (6)$$

The relative velocity of the ground target in the projectile coordinate system is represented by formula (7).

$$v_r = Q^T \begin{bmatrix} v_m \\ 0 \\ 0 \end{bmatrix} - \begin{bmatrix} 0 \\ v_t \\ 0 \end{bmatrix} \quad (7)$$

where Q^T represents the transpose matrix of the rotation matrix, v_m represents the ground target's velocity, and v_t represents the projectile's flying velocity.

If the position of the target in the projectile coordinate system is known, considering the relative velocity between the projectile and the target, as well as the target size, a constraint function of the ground target detected by the system is established for the system, as shown in formula (8).

$$\begin{cases} z_t^2 + y_t^2 = \pi D^2 / 4 \\ t_{\max} = \frac{R}{v_r} \end{cases} \quad (8)$$

where (x_t, y_t, z_t) represents the position of the target in the projectile coordinate system after a certain duration time that laser irradiates on the ground target, $[x_t \ y_t \ z_t]^T = [x_0 \ y_0 \ z_0]^T + v_r t_{\max}$, $[x_0 \ y_0 \ z_0]^T$ is the initial position of the target in the projectile coordinate system, R is the distances from the system to the ground target. If the ground target is defined as a rectangular prism, its width is D . To determine whether there is an intersection between the laser beam and the surface of the ground target, if there is an intersection within t_{\max} and the distance from the intersection point to the origin of the laser beam is within the maximum detection distance, then the pulse laser beam is considered to have detected the target.

In order to study the detection performance of the

laser fuze circumferential detection system, the constraint function of the effective intersection of the projectile and target is given based on the coordinate conversion between the laser fuze and the target. On the premise that the target is detected by laser fuze, echo power calculation mathematical model and signal processing method of laser fuze based on circumferential detection mechanism are studied.

4. Echo power calculation mathematical model and signal processing method of laser fuze based on circumferential detection mechanism

4.1. Echo signal processing method based on minimum mean square adaptive filtering

When the laser fuze circumferential detection system detects the ground target under the condition of cloud and fog environment, due to the short time interval between the scattering echo and the target echo, the two types of echo signals superimpose, leading to distortions such as signal broadening in the detected echo signals. Additionally, the uncertainty factors caused by external natural environment, such as cloud and fog interference, introduce random variations in the strength and timing of the interference signals. The characteristic parameters of the interference signals cannot be quantitatively described. Therefore, filtering processing is required to handle the random interference signals and ensure the system's detection performance [20-21].

Considering the real-time nature of laser detection and the limitations of system size and power consumption, the minimum mean square adaptive filtering method is adopted to filter out the interfere signals under cloud and fog interference [22]. The mixed signal $T_r(n)$ of the target echo signal $T(n)$ and the cloud and fog interference signal $R(n)$ is applied as one input to the adaptive filter, while the estimated reference input of the cloud and fog interference signal is used as the other input. The input signal $T_r(n)$ is filtered taking the adaptive filter, which adjusts its output signal $q_{out}(n)$ to match signal $R(n)$. The output error $\Delta e(n)$ represents the best estimate of the target echo signal. The principle of least mean square adaptive filtering is shown in Fig. 4.

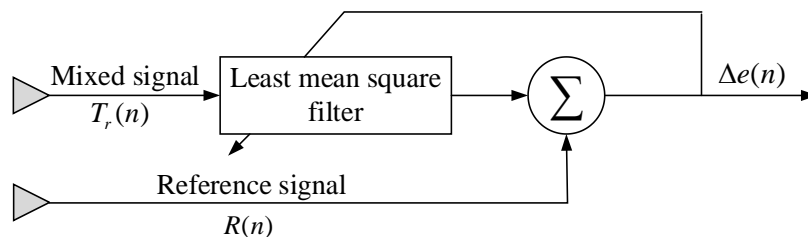


Fig. 4. The principle of least mean square adaptive filtering

Assuming the lengths of the mixed signal $T_r(n)$ and the target echo signal $T(n)$ are M , and the number of filter taps is N , the value range of n is $[N, M]$. The iterative process is shown in formula (9).

$$F(n+1) = F(n) + 2\kappa \bar{T}_r(n) \Delta e(n) \quad (9)$$

where, $\bar{T}_r(n)$ represents the vector of the mixed signal, and $\bar{T}_r(n) = [T_r(n), T_r(n-1), \dots, T_r(n-N+1)]$ and $F(n)$ is the weight vectors of the filter taps, $F(n) = 0$, κ is the iterative step size factor, $\Delta e(n)$ is error, $\Delta e(n) = F(n) - q_{out}(n)$, $q_{out}(n) = F(n)^T \bar{T}_r(n)$. The filter weight vectors are updated in real-time based on the error, enabling adaptive filtering of the signal. In addition, the basic principle of adopting the variable step size algorithm is to dynamically adjust the step size factor by establishing the nonlinear relationship between the step size factor and the error, so that the algorithm can take into account the convergence speed and steady-state error [23-24].

To achieve fast convergence and steady-state error, a variable step size algorithm with step size memory effect is employed, considering the characteristics of the cloud and fog interference signal. In the algorithm, the step size factor is given by formula (10).

$$\kappa(n) = c_4 \kappa(n-1) + c_4 c_3 \tanh[c_2 |\Delta e(n)|^{c_1}] \quad (10)$$

where, $c_1 \sim c_5$ are the step size control parameter, $b(n)$ is defined as the step size function, and $b(n) = c_3 \tanh[c_2 |\Delta e(n)|^{c_1}]$. Formula (10) is a model of step size factor in the variable step size algorithm with step size memory effect, which is related to step size control parameters and errors. In order to realize dynamic parameters instead of fixed parameters, step size control parameters are used to adjust step size factors. The convergence speed is dynamically adjusted according to the difference between the current error signal and the previous error signal, and the irrelevant noise is suppressed.

The influence of the different step size parameter on the step size factor is discussed; the convergence performance of the algorithm under different step-size control parameters is described. When $c_2 = 2$, $c_3 = 0.5$, $c_4 = 0.7$, $c_5 = 0.4$, c_1 are set to 0.5, 1, 2, 3, and 4, respectively, Fig. 5 shows the relationship curve between the different step size control parameters and error.

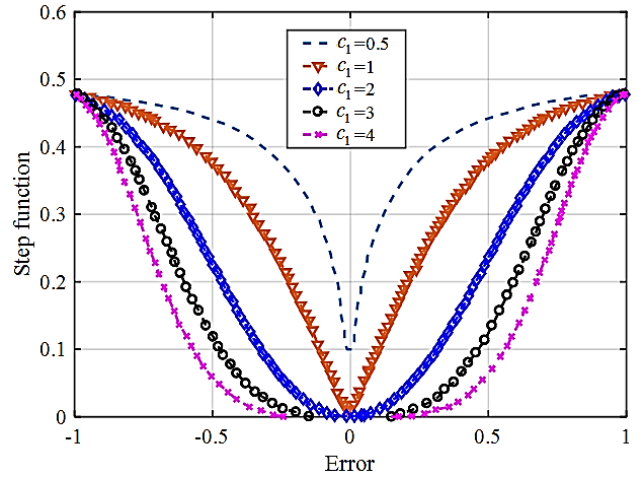


Fig. 5. The relationship between different step size control parameters and error (color online)

In Fig. 5, when $c_1 = 0.5$, and the error approaches 0, the step size function converges sharply, resulting in significant steady-state error. As the value of c_1 increases, when the error approaches 0, the convergence speed of the step-size function becomes slower, until $c_1 = 4$, when the error is approximately 0.2, the step size function becomes 0. This indicates that when the error is still changing, the step size function no longer changes. This situation can lead to significant steady-state error and steady-state misalignment. It also can be found that different values of c_1 have a significant impact on the convergence speed and bottom shape of the step-size function. Choosing appropriate step-size parameters and combining convergence characteristics is beneficial for tracking and reducing steady-state error.

When $c_1 = 2$, $c_2 = 3.4$, $c_3 = 0.5$, $c_5 = 0.4$, c_4 are set to 0.6, 0.7, 0.8, and 0.9, respectively, Fig. 6 presents the variation curve of the algorithm's convergence performance with respect to c_4 .

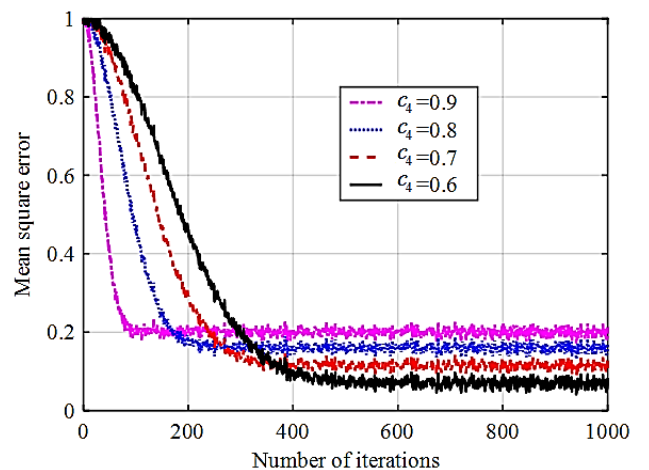


Fig. 6. The impact of a_4 on the convergence performance of the algorithm (color online)

From Fig. 6, it can be observed that the convergence performance of the algorithm varies with different C_4 values. Although the convergence speed of the algorithm improves as the value of C_4 increases, the convergence accuracy decreases.

4.2. Echo power calculation mathematical model

The circumferential emission laser beam state is formed by the laser fuze as the projectile rotates, and the echo energy reflected by the ground target is received by the photodetector to achieve the detection of the system. Assuming the bidirectional reflection distribution function $f_r(\gamma)$ on the target surface represents the ratio between the irradiance of the target's surface reflection direction and the irradiance of the incident direction [25-26], as shown in formula (11).

$$f_r(\gamma) = \frac{M'}{\cos^6 \gamma} e^{-\frac{\tan^2 \gamma}{m^2}} + N' \cos^{n'} \gamma \quad (11)$$

where, the first term represents the specular reflection component of the target's surface, and the second term represents the diffuse reflection component of the target's surface. M' is the amplitude of specular reflection, N' is the amplitude of diffuse reflection, m is the slope of the target's surface, and n' is the diffuse reflection coefficient.

Assuming the surface reflection characteristics of the ground target are consistent, the radar cross-section equation of the ground target detected by the system is represented by formula (12).

$$\phi = 4\pi f_r(\gamma) \cos^2 \gamma A_t \quad (12)$$

where A_t is the area of the scattering cross-section, and γ is the reflection angle of the target's surface. Due to the narrow field of view of the laser fuze circumferential detection system, when the intersection conditions between the projectile and the target is the close-range, it can be assumed that the reflection angle γ formed by laser incidence at any position on the target's surface within the detection field is constant,

$\cos \gamma = \frac{R \cos \varpi}{\sqrt{R^2 + y_m^2}}$, among, ϖ is the angle between

the field of view's central axis and the vertical direction.

In the time domain, the pulse laser emitted by the laser follows a Gaussian distribution, and the laser emission power is represented by formula (13).

$$P_i(t) = P_0 e^{-\frac{t^2}{\tau^2}} \quad (13)$$

where P_0 is the peak of the laser emission power, τ is the pulse width of the laser. The pulse laser has a half-width at half maximum of $2\tau\sqrt{\ln 2}$.

The echo power received by the system from the target's surface is given by formula (14).

$$P_e = \frac{P_0 e^{-\frac{t^2}{\tau^2}} \xi}{4\pi R^2} \frac{4\pi f_r(\gamma) A_r}{4\pi R^2} \frac{R \cos \theta}{\sqrt{R^2 + y_m^2}} A_r \eta_1^2 \eta_2^2 \quad (14)$$

where ξ is the emission optical gain of the laser, A_r is the laser optical receiving area of the system, η_1 is the atmospheric transmittance. Since the system operates in a close-range detection mode, the atmospheric transmittance can be considered approximately constant. η_2 is the optical transmittance of the system.

5. Calculation and analysis

The effect of different pulse width laser echoes on the minimum mean square adaptive filtering is computed and analyzed in the presence of cloud and fog interference. The echo signal amplitude is set to 6.1 V in the absence of cloud and fog, with a pulse width of 5 ns. The cloud and fog interference signal has amplitude of 3.4 V and pulse widths of 4 ns, 10 ns, 16 ns, and 20 ns. The peak of the cloud and fog interference signal occurs 10 ns after the peak of the echo signal in the absence of cloud and fog. The simulated signals are shown in Fig. 7(a). The echo signal processed adopting the minimum mean square adaptive filtering method is shown in Fig. 7(b). Comparing Figs. 7(a) and 7(b), it is observed that the interference signal amplitude is compressed to approximately 0.4 V after filtering. The widening of the echo signal width and its peak effect are reduced, thereby improving the signal restoration and the processing accuracy of the algorithm.

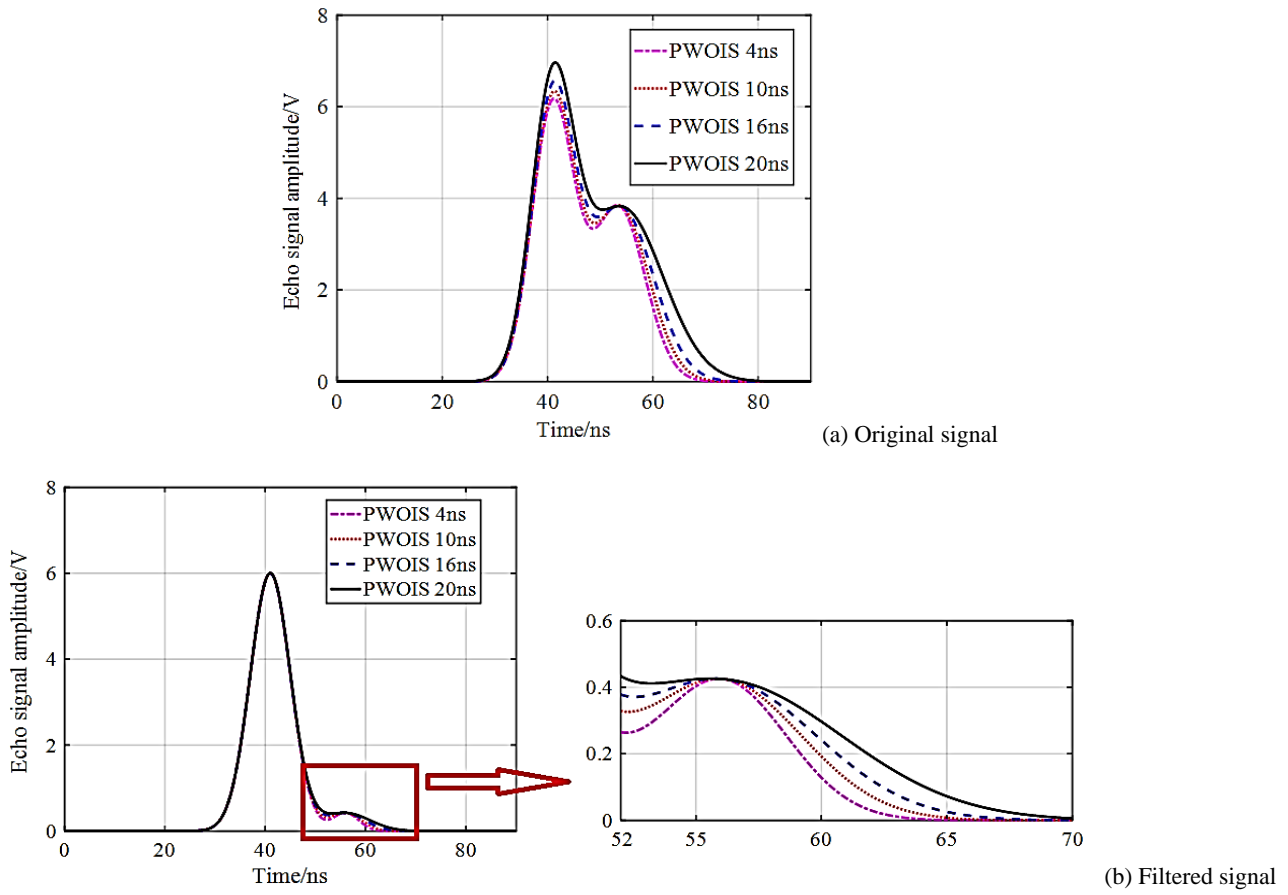


Fig. 7. The change curve of filtering effect of laser echoes with different pulse widths in a cloud and fog environment (color online)

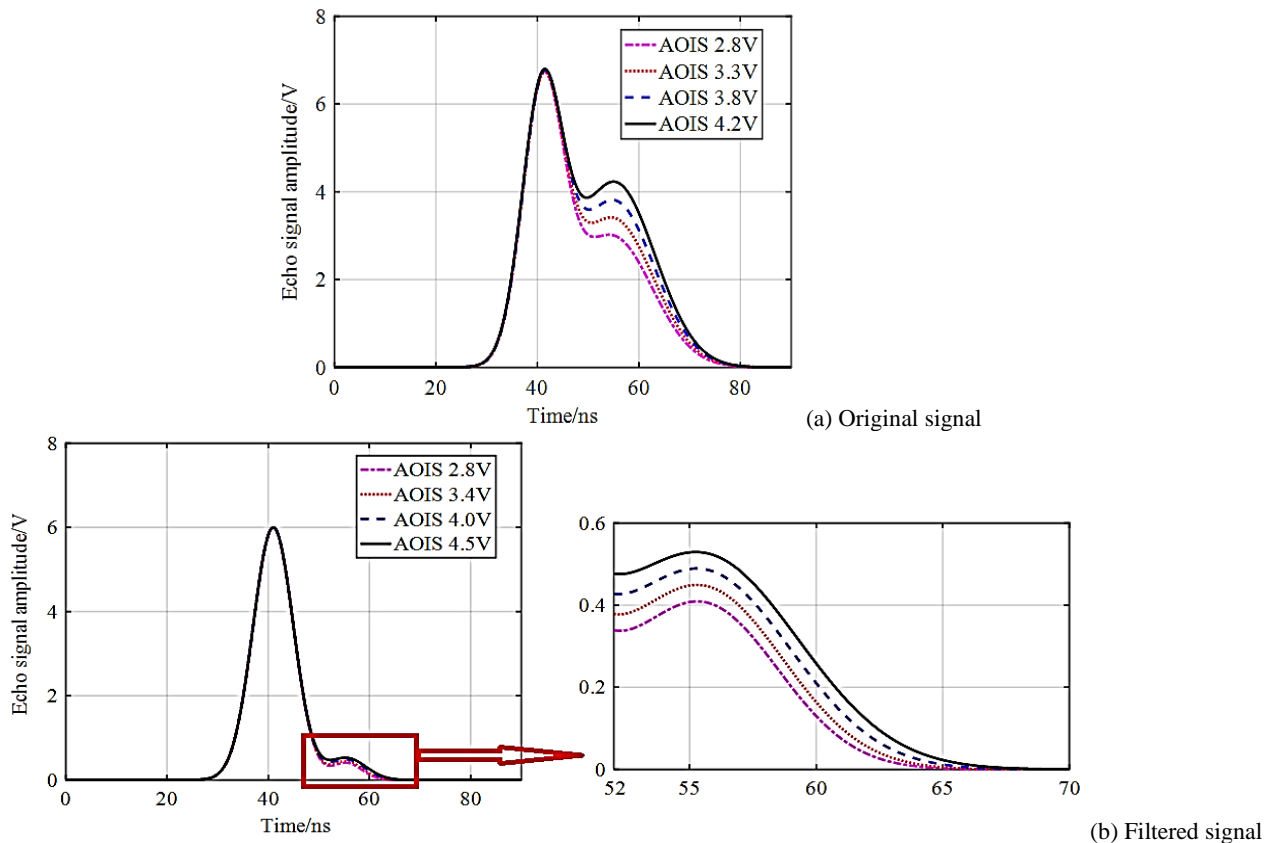


Fig. 8. The change curve of filtering effect of different energy interference echo signal in a cloud and fog environments (color online)

The visibility of cloud and fog can also cause fluctuations in the energy of the interference signal. The effect of different energy levels of the interference signal on the minimum mean square adaptive filtering is calculated and analyzed. In the absence of cloud and fog, the parameters of the echo signal remain unchanged, while the pulse width of the cloud and fog interference signal is 16 ns, and the amplitudes are 2.8V, 3.3V, 3.8V and 4.2V. The peak of the cloud and fog interference signal occurs 10 ns after the peak of the echo signal in the absence of cloud and fog. The simulated signals are shown in Fig. 8(a). The echo signal processed employing the minimum mean square adaptive filtering method is shown in Fig. 8(b). Comparing Figs. 8(a) and 8(b), it is observed that the amplitude of the filtered interference signal increases with the increase of the original peak value. The widening of the echo pulse width and its peak effect are alleviated. It verifies that the filtering method proposed in this paper can effectively filter out the cloud and fog interference signals with different energy levels.

The presence of fog in the natural environment introduces randomness, causing uncertainty in the occurrence of foggy interference signals. The influence of different timings of foggy interference signal occurrences on adaptive filtering methods is investigated. The echo parameters remain unchanged in the absence of fog. The foggy interference signals have a pulse width of 16 ns and amplitude of 3.1 V. The simulated signals are observed to occur 35 ns before the peak of the echo signal, 25 ns before the peak, 25 ns after the peak, and 35 ns after the peak, respectively, as shown in Fig. 9(a). The echo signal processed using the minimum mean square adaptive filtering method is presented in Fig. 9(b). The results indicate that the interference signal amplitudes for different timings of foggy interference are suppressed below 0.43 V. The effective part of the echo signal containing cloud and fog interference signal and the echo signal without cloud and fog interference. Therefore, the filtering method proposed in this paper can effectively reduce foggy interference signals at different timings.

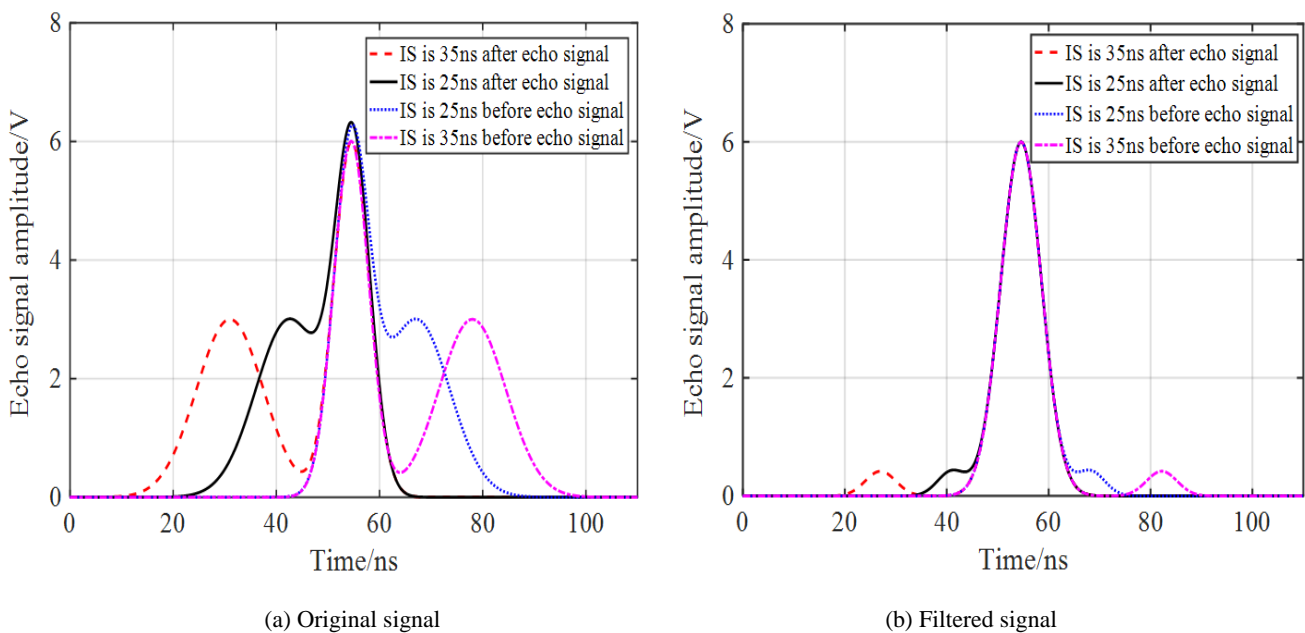


Fig. 9. The change curve of filtering effect of echo signal at different timings in a cloud and fog environments (color online)

The detection probability of the system under different laser pulse frequencies and motor scanning speeds was analyzed through Monte Carlo simulation. Assuming the projectile and target are in a close range intersection state, the ground target has a length of 5 m and a diameter of 2 m. The maximum detection distance for the laser fuze is set to 5 m, and the projectile's velocity is $v_1 = 300$ m/s, focusing solely on the detection probability when the projectile could detect the ground target. The motor speed, denoted as $n_2 \in [5000, 15000]$, the speed is

varied in steps of 1000, and the pulse frequency, denoted as $f \in [1000, 5000]$, and which is varied in steps of 500. Different combinations of n_2 and f are selected for each simulation to investigate the detection probability of the system at different scanning angles. When $v_2 = 50$ m/s, the relationship between detection angle, pulse frequency of the laser, motor speed, and detection probability of the system is illustrated in Figs. 10(a) and 10(b).

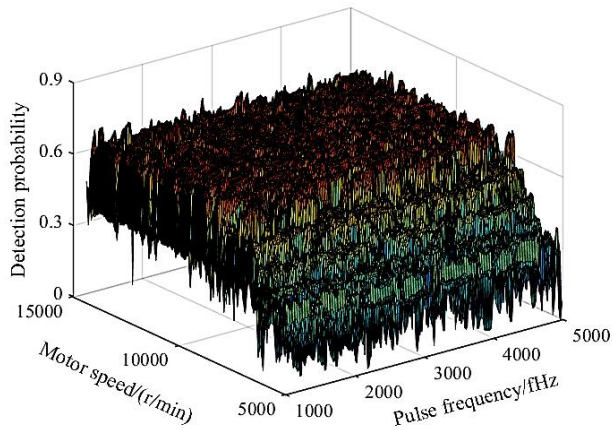
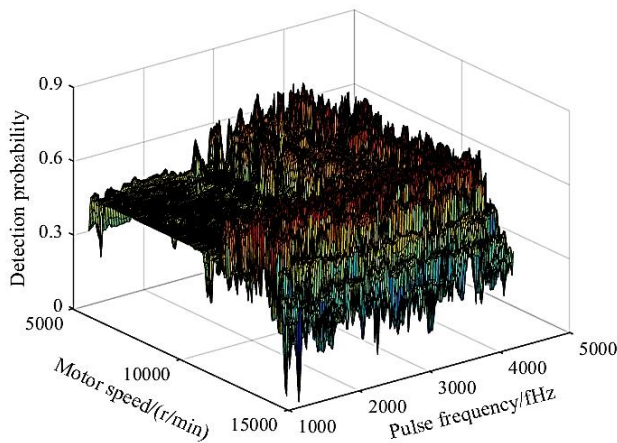
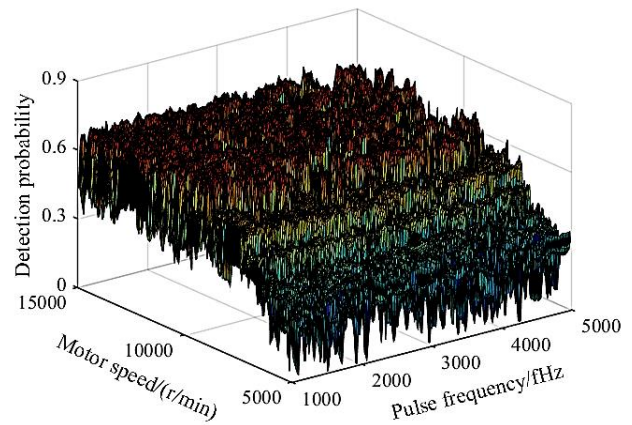
(a) $\varphi = \pi/3$ (b) $\varphi = \pi/6$

Fig. 10. The detection probability of the system at different detection angles (color online)

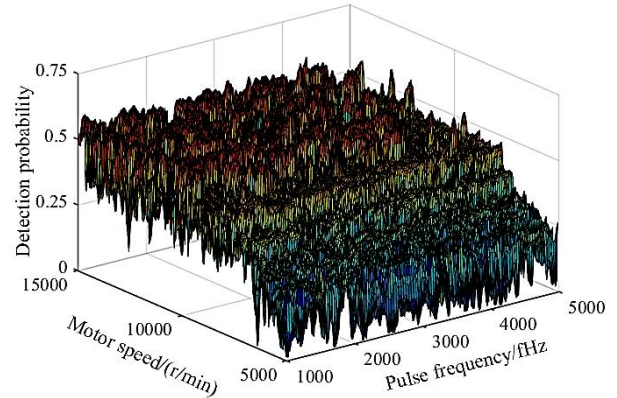
When pulse frequency of the laser is less than 2kHz, as the motor speed increases, the detection probability of the system remains relatively constant. If only the motor speed is increased, even if the motor speed is very high, the detection probability of the system will not significantly increase because the motor speed and pulse frequency do not match. When the pulse frequency of the laser is greater than 2kHz, the detection probability of the system increases with the increase of motor speed. When the motor speed is greater than 10000r/min, the detection probability of the system begins to converge, and the detection probabilities converge to 0.736 and 0.823 when the detection angles are $\pi/3$ and $\pi/6$, respectively. Comparing Figs. 10(a) and 10(b), the detection probability of the system increases with an increase in detection angles. By increasing the detection angle, that is, the intersection angle of the projectile and the target is increased, the detection probability of the system can be effectively improved.

When the intersection angle of the projectile and the

target is $\pi/6$, the relationship between ground target's velocity, pulse frequency of the laser, motor speed, and detection probability of the system is depicted in Figs. 11(a) and 11(b). It can be observed that as the ground target's velocity increases, the detection probability of the system gradually decreases and the convergence interval shifts towards higher pulse frequency of the laser and motor speed. When the ground target's velocity increases, in order to maintain the detection probability of the system, it is necessary to increase the motor speed and pulse frequency of the laser.



(a) Target's velocity is 50 m/s

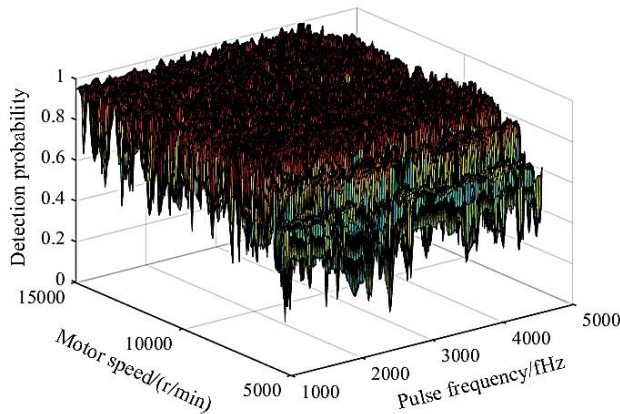


(b) Target's velocity is 70 m/s

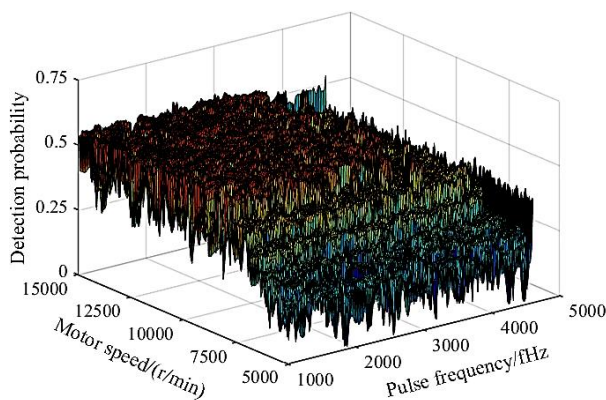
Fig. 11. The detection probability of the system under different target velocities (color online)

When the intersection angle of the projectile and the target is $\pi/6$, Fig. 12 presents the detection probability of the system at different detection distances. Under the same conditions of motor speed and pulse frequency of the laser, the detection probability of the system decreases with an increase in detection distance. Even when the motor speed and pulse frequency of the laser reach their maximum, the detection probability of the system remains low. This is because as the detection distance increases, the scanning angle available to the detection system decreases,

reducing the spatial range of laser circumferential scanning. Additionally, as the detection distance increases, the attenuation of the laser echo signal reduces the probability of the system detecting the target.



(a) Detection distance is 3.5 m



(b) Detection distance is 7 m

Fig. 12. The detection probability of the system under different detection distances (color online)

In order not to miss the target in a single scanning period, the scanning frequency of the system must meet the minimum scanning frequency based on the laser fuze circumferential detection system. At the same time, the scanning frequency of the system has a certain influence on the detection ability of the system. Without changing the scanning frequency of the system, in order to improve the detection ability of the system, improve the emission power of the laser, increase the optical area of the laser receiving module, use the lens with higher optical transmittance, and adjust the wavelength of the laser. Its main purpose is to improve the energy of the echo signal obtained by the system under the same detection distance, and provide the premise for the system to detect the target, and then combine the signal processing method to make the system identify the target accurately. The research results of this paper provide valuable reference for the reliable detection and precise strike of laser fuze detection system.

6. Conclusions

Based on the working principle of dual-transmitter and dual-receiver laser fuze circumferential detection system, a projectile-target intersection model is established in the ground target coordinate system. In order to improve the detection probability of the system, the critical conditions for the motor scanning frequency and pulse frequency of the laser to detect targets are derived. In order to filter out the impact of external environmental interference, a variable step size filtering method with step size memory effect is designed based on the least mean square adaptive filtering principle. By utilizing the bidirectional reflectance distribution function, echo power calculation mathematical model is deduced. These random interference factors, namely pulse width, peak power, and echo time, are analyzed to verify the anti-interference performance of the filtering method, the simulation analysis reveals that the detection probability of the system is influenced by factors such as the intersection angle of projectile and target, detection distance, and target's velocity. The established calculation model can provide a reference basis for improving the detection performance of laser circumferential detection systems under various intersection conditions.

References

- [1] Yuzhao Li, Yan Liu, Xi Chen, Sha Sha, Juan Guo, *Infrared and Laser Engineering* **47**(12), 36 (2018).
- [2] Lin Gan, He Zhang, Xiangjin Zhang, *Acta Armamentarii* **34**(8), 942 (2013).
- [3] Hanshan Li, Xiaoqian Zhang, Xuewei Zhang, Quanmin Guo, *Defence Technology* **18**(8), 1405 (2022).
- [4] Wei Zhang, Yuzhao Li, Zhesi Wang, Yan Liu, *Infrared and Laser Engineering* **49**(4), 58 (2020).
- [5] Bingting Zha, Hailu Yuan, Shaojie Ma, Guangsong Chen, *Acta Physica Sinica* **68**(7), 79 (2019).
- [6] Xiaobin Xu, He Zhang, *Chinese Journal of Lasers* **43**(5), 201 (2016).
- [7] Lixin Yao, Xiaoyao Zhao, Shuaixiang Wang, Yongqiang Yu, *Acta Armamentarii* **43**(1), 218 (2022).
- [8] He Zhang, Hongxia Li, Libo Ding, Bingting Zha, *Infrared and Laser Engineering* **49**(4), 9 (2020).
- [9] Bangfu Ni, Hongqing Qian, Kui Zhou, *Tactical Missile Technology* **36**(6), 85 (2015).
- [10] Xiangsheng Meng, Lekun Li, *Infrared and Laser Engineering* **52**(4), 309 (2023).
- [11] Zuntian Chen, Linshan Geng, Ruiqi Chen, *Journal of Detection and Control* **44**(2), 1 (2022).
- [12] Tao Feng, Xiangjin Zhang, Zongchen Yao, *Applied Laser* **39**(2), 322 (2019).
- [13] Akira Higuchi, Hideyuki Naito, Kousuke Torii, Masahiro Miyamoto, Takenori Morita, *Optics Express* **20**(4), 4206 (2012).
- [14] Zao Cheng, Min Xia, Wei Li, Wenping Guo, Xianjing Zeng, Kecheng Yang, *Laser and Optoelectronics Progress* **53**(1), 38 (2016).

- [15] Hanshan Li, Xiaoqian Zhang, Junchai Gao, IEEE Sensors Journal **22**(22), 21600 (2022).
- [16] Xiaoqian Zhang, Hanshan Li, Microwave and Optical Technology Letters **62**(7), 2463 (2020).
- [17] Hanshan Li, Xiaoqian Zhang, Xuwei Zhang, Liping Lu, Measurement **177**, 109281 (2021).
- [18] Stefania Matteoli, Giovanni Corsini, Marco Diani, Giovanna Cecchi, Guido Toci, IEEE Transactions on Geoscience and Remote Sensing **53**(1), 375 (2015).
- [19] Kun Zhong, Wei Su, Bo Peng, Shaling Huang, Zhongyun Li, Infrared and Laser Engineering **49**(2), 46 (2020).
- [20] Songlang Li, Zhongyang Mao, Chuanhui Liu, Min Liu, Opto-Electronic Engineering **47**(3), 190389 (2020).
- [21] Lin Gan, He Zhang, Chinese Journal of Lasers **49**(7), 40 (2022).
- [22] Guillaume Schimmel, Thomas Produit, Denis Mongin, Jérôme Kasparian, Jean-Pierre Wolf, Optica **5**(10), 1338 (2018).
- [23] Meng Wang, Jianping Zhao, Bingting Zhang, Communications Technology **49**(6), 668 (2016).
- [24] Po Yang, Zhuhua Liu, Shipboard Electronic Countermeasure **40**(4), 59 (2017).
- [25] Qi Zhao, Guangyu Du, Bin Zhang, Yanbin Zhai, Yuruo Shi, Journal of Systems Engineering and Electronics **28**(3), 572 (2017).
- [26] Shanshan Chen, He Zhang, Xiaobin Xu, Acta Armamentarii **39**(6), 1095 (2018).

*Corresponding author: wujie198866@163.com